

Optimization the Performance of a Synchronization Controller For a 3-Phase Photovoltaic Grid-Connected System Using the PSD Algorithm

GHITA BENNIS*, MOHAMMED KARIM*, AHMED LAGRIOUI**, MERYEM FELJA*

*LISTA Laboratory, Faculty of Sciences Dhar El Mahraz, Sidi Mohammed Ben Abdellah University Fès, MAROCCO

**Department of Electrical Engineering And Computer Engineering, National School of Arts and Métiers, University Moulay Ismail Meknes – MAROCCO

Abstract: - In a distributed generation system, divers renewable agents are connected to the low voltage 3 phase utility grid by an inverter which is used as power condition and must assurance the higher efficiency of the renewable agent. To achieve this level of efficiency, a unitary power factor between the utility grid voltages and the inverter currents is necessary, and a synchronization algorithm is required for the perfect synchronization between the 3-phase utility grid and the renewable agent. The aim of this paper is to present the optimization of the performance of a Synchronization controller for a 3-phase photovoltaic grid-connected system, assessing its accuracy under different conditions and studying their drawbacks and advantages. A grid connected photovoltaic system with a nominal power of 5 kW is used so as to assess the behavior of the synchronization algorithm when the 3 phase utility grid is affected by some disturbances such as voltage unbalances

Key-Words: - PV Array, PSD, PLL, Inverter, MPPT,...

1 Introduction

Solar energy has become the most popular renewable energy source where in energy is extracted directly from sun employing photovoltaic modules [1-4]. The power electronics converters, variable nonlinear loads and voltage regulators inject harmonics to the grid and are accountable for serious power quality problems [5]. Indeed, there are a number of outstanding problems mainly related to the power quality, such as reactive power compensation, power factor, harmonics and voltage regulation in a photovoltaic system connected to grid [6]. The global performance of the total system gets affected and it becomes a serious concern for the final users. Any integration of renewable energy sources to the grid has to meet standard power quality requirements. The power quality expected from distributed generations has been the subject of discussion and standardization. In a Photovoltaic system, the signal quality is of particularly preoccupied due to high proportion of nonlinear and single-phase loads. moreover, switching of a single-phase load can depict a large transient leading to sag

and swell of voltage signal. generally, the grid connected Photovoltaic system fails to control harmonic currents and the reactive power drawn by the nonlinear load. mostly passive filters are used to control the harmonics currents generated. But due to divers disadvantages like series/parallel resonance, these filters have been changed and also these filters are not suitable for certain loads [7]. Active power filter is a better choice which ameliorates harmonic compensation features of the passive filter. In this works new control algorithms have been designed focusing on increasing the performance of the connection of primary renewable energy agents to the low voltage 3 phase utility grid. It is essential an appropriated control of the power factor of the inverter grid connection to get the maximum efficiency in the photovoltaic agent, and the synchronization algorithm will be one of the aim modules in detecting the phase angle of the 3 phase utility grid voltages with optimal dynamic response. the Synchronous Reference Frame Phase Locked Loop (dqPLL method) is the classical synchronization algorithm, in view of it is easy to implement, but it is also very sensible to grid voltage unbalances leading to errors when the

frequency and phase are detected. For this, a big amount of studies has been carried out in this area in order to discover a solution to this fact, as may be found in [8–14], the most of them showing a perspective of how to solve this issue when the detection of the frequency is conducted.

2 GRID Connected Photovoltaic System

This document focuses on the photovoltaic systems granted to the network, an "intelligent" voltage control system integrated in PV inverters is proposed. It ensures that the voltage inverters of PV inverters can withstand the voltage dips on the network. The proposed system decrease connection costs and upgrade the performance of grid-connected PV inverters. On the other hand, a control / control system for limiting overvoltages of the DC bus of the PV inverters is developed. This system avoids failures and connections of PV systems in the event of a short circuit [3].

3 Power Subsystem

The power subsystem is constituted by the Photovoltaic array, a converter (DC-DC) controller by MPPT, and inverter (DC-AC) and the LCL filter. ensuing, a brief description of each block is developed.

3.1. Photovoltaic modules

A photovoltaic generator consists of an elementary PV cell assembly mounted in series and / or parallel to obtain desired electrical characteristics such as power, short-circuit current and open voltage. This generator allows a suitable conversion of solar energy into solar electric energy in the form of tesion and direct current, variable according to the influence of temperature and illumination [4].

3.2. The converter controller by MPPT

The boost converter is used not only to uplift the Photovoltaic array output voltage, but also to realize Perturb and Observe (P&O) scheme in Maximum Power Point Tracking (MPPT) [5,25]. The boost converter connected to Photovoltaic array, forever works in a continuous current mode and the current ripple is reduced by using a large value of inductor. A low value of capacitor at output acts as filter.

3.3. The inverter

The inverter acts as a control of the output current and indirectly of the DC bus voltage. The control diagram of the inverter is shown in Figure 1, it consists of two parts with two different roles: control of the output current (internal loop) and control of the DC bus voltage (external loop) via the command of The output power of the inverter [6]. The SVM and PWM techniques are employed to control the grid signals of the commutator according to the average voltage and the current references [7].

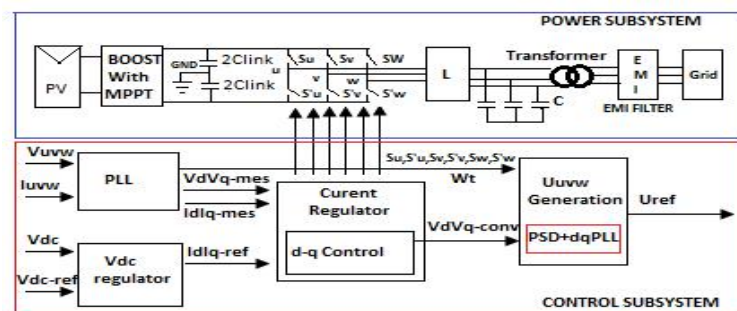


Figure 1. Block diagram of the power and control subsystems for the 3-phase grid-connected PV system.

$$i_p = i_{link} + i_{cc}$$

$$i_{cc} = S_u \cdot i_u + S_v \cdot i_v + S_w \cdot i_w \tag{1}$$

$$i_{link} = C_{link} \left(\frac{dV_{cc}}{dt} \right)$$

$$P_{pv} = i_p V_p$$

Where v_p , i_p are the voltage and the output current of the photovoltaic generator, respectively, PPV is the power available for a specific irradiation, V_{cc} is the DC bus voltage, link i_c is the current through the link capacitor C_{link} , And i_{cc} is the current delivered to the phase 3 VSI (which is a function of the line currents i_u , i_v , i_w and the states of the power poles S_u , S_v , S_w (1: -upper Pole, If the lower pole in the 3-phase VSI.) as a result of the fact that the voltage in the capacitor is roughly the same as the voltage in the three-phase grid, the dynamics in the ac of the inverter expressed. in a vector the following way is the following:

$$u - u_{AC} + L \frac{di}{dt} = u_R + u_L \tag{2}$$

Where U is the voltage of the inverter, i : line current of the inverter, U_{ac} : vectors of the service grid voltage space, L : line inductance, R : resistance. By expressing the last vector equation with its

components d and q in the dq axes using the transformation of the Park vector [9,16], the instantaneous active power (p) and the instantaneous reactive power (q) can be expressed as follows [8, 16]:

$$P = U_{ACd} i_d + U_{ACq} i_q \quad (3)$$

$$q = U_{ACd} i_q - U_{ACq} i_d \quad (4)$$

Where U_{ACd} , U_{ACq} , identifies the d - q mechanisms of the three-phase voltages and currents, respectively, permitting decoupled control of the instantaneous active and reactive powers if the vector U_{ac} is aligned with the d -axis ($U_{ACq} = 0$).

3.4. LCL Filter

In order to be able to connect the voltage inverter in parallel with the mains, and to make it work as a current source, it is necessary to use an inductive connection filter (L or LCL). Whatever the filter used for the connection, one will always have the same schema equivalent: a controlled source (discontinuous alternative in the case of the topology L , is quasi sinusoidal with the topology LCL) which is known to the network through an inductor [10-16].

3.5. EMI filter

In a grid-connected renewable agent, it is essential to take into consideration, the harmonic pollution due to the Electromagnetic Interference (EMI). These EMIs are generated, by the commutation of semiconductor electronic devices (IGBTs and diodes) [20] and an EMI filter is necessary to reduce it. There are various methodologies to design an appropriate EMI filter, some of them are founded on trial and error [17,18], and some novel methodologies are cited in several publications, including [17,19].

4 Control Subsystem

The control subsystem is formed by the PI regulators, PSD synchronization, and the u_{vw} generation.

4.1. PI REGULATORS

A three-phase PV system is modeled by a current injector with its power regulation. The control system regulates the power injected by the PV system into the connection node as a function of the

sunshine.

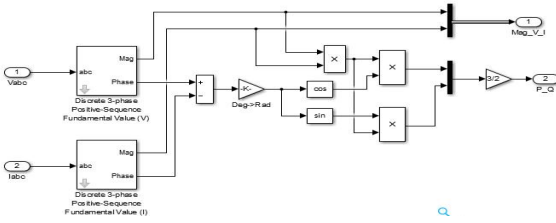
The operation of this model can be designated by (FIG. 1): from the voltages and currents measured at the point of connection of the injector, the active and reactive powers which regulate it are determined. These powers are controlled by simple Proportional-Integral type correctors ($K_p + K_i / p$). The current references are then calculated in the Park repository by the formula:

$$I_d = \frac{2(P.V_d + Q.V_q)}{3(V_d^2 + V_q^2)} \quad (5)$$

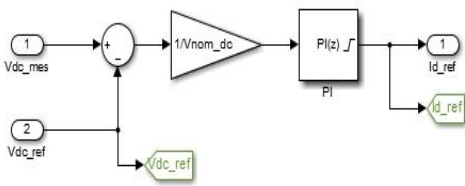
$$I_q = \frac{2(P.V_d - Q.V_q)}{3(V_d^2 + V_q^2)} \quad (6)$$

Where P and Q are the reference powers of the PV system. V_d et V_q are the direct and quadrature components of the voltage, measured at the connection point of the PV system, in the Park repository. I_d et I_q are the direct and in quadrature components of the reference product current by the PV system on the network to which it is connected. These currents therefore depend on the power requirements and on the voltage measured at the point of connection of the production. A Phase Locked Loop (PLL) is used to synchronize the Park transformation to the pulsation of the measured voltage across the network. Thus, when the system is in steady state, the direct component V_d en output from the Park transformation is an image of the amplitude of the measured voltage and the quadratic component V_q is zero. These currents are then converted into the three-phase frame of reference [20]. The amplitude and the phase shift of the currents injected into the network will thus regulate the powers to their set value. The limit for the component I_d is chosen as a function of the maximum output current of the inverter and the power limit of the DC source (for example $I_{dmax} = 1.1 I_n$). The limit for the I_q component is chosen accordingly, so as not to exceed the selected reactive power limit (eg $Q / P = 0.4$). Two PI correctors are in charge of regulating the active and reactive powers to their setpoint. Thus, there are two loops: the loop for regulating the active power and the loop for reactive power. Considering that the selected Park reference frame rotates at the voltage pulse, then it is possible to set $V_q = 0$ and $V_d = V_{max}$. Thus, the active power control loop can be modeled as shown in Figure 2 (b) with ε which

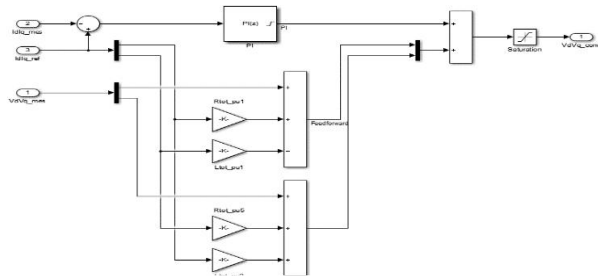
represents the difference between the setpoint power and the measured power (error term). By considering $V_q = 0$ and V_d constant [21].



(a) bloc diagram of PSD



(b) bloc diagram of Vdc regulator



(c) bloc diagram of current regulator

Figure 2. (a,b,c,) bloc diagram of controller for 3-phase VSI for PV system

The design of the Phase Locked Loop gain is a critical point within this process. The closed loop transfer function of the dqPLL is giving by:

$$H(s) = (K_p s + K_i) / (s^2 + K_p s + K_i) \quad (7)$$

where K_p is the proportional gains employed PI regulator, K_i : integral gains of the employed PI regulator. Eq. (7) is a second order transfer function, similar to (8).

$$G(s) = (2\xi\omega_0 s + \omega_0^2) / (s^2 + 2\xi\omega_0 s + \omega_0^2) \quad (8)$$

where ω_0 is the natural angular frequency, ξ : is the damping factor. from equating (7) and (8):

$$K_p = 9.2 / T_s \quad (9)$$

$$\omega_0 = K_p / 2\xi \quad (10)$$

$$K_i = \omega_0^2 \quad (11)$$

In this work, the dqPLL gains are calculated so as to obtain $T_s = 0.05$ ms (one 50 Hz cycle) allowing a fast response of the algorithm when a variation of the nominal frequency occur, and a damping factor $\xi = 0.871$ is chosen. Equating (9)– (11), another variable can be computed: $K_p = 60$, $\omega_0 = 37.41$ rad/s and $K_i = 1400$. The value give of ω_0 guarantees a trade-off between the dynamic, the stability and harmonic rejection capability of the dqPLL algorithm.

The PLL method is very sensitive to the grid voltage unbalance [22], which also produces second order harmonics in d–q synchronous reference frame due to the effect of the inverse sequence, in fact, the sensors to be utilized can introduce second order harmonics due to accuracy errors. moreover, the 3 phase low voltages of the utility grid could be contaminated with harmonics and assumed by variations of the fundamental frequency. A resolution to the problems caused by the unbalance 3 phase utility grid voltages is adding a PSD block, which is founded on the symmetrical components method [23]. In order to have a good performance of the PLL algorithm, it is possible to decompose the unbalanced 3-phase utility network voltages into negative, positive and zero sequences. In time domain, the instantaneous positive sequence component V_{+abc} of a voltage vector is given by [24]:

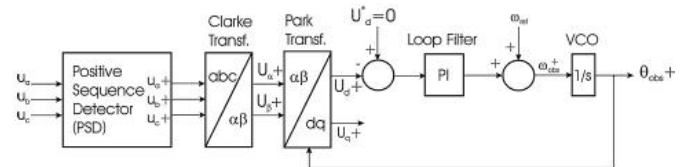


Figure 3. Block diagram of the PSD + dqPLL synchronization algorithm.

$$V_{a+}(t) = 0.5 V_c(t) - ((1/6)(V_b(t) + V_c(t)) - (1/2\sqrt{3})S_{90}(V_b(t) - V_c(t))) \quad (12)$$

$$V_{b+}(t) = -(V_{a+}(t) + V_{c+}(t)) \quad (13)$$

$$V_{c+}(t) = 0.5 V_b(t) - ((1/6)(V_a(t) + V_b(t)) - (1/2\sqrt{3})S_{90}(V_a(t) - V_b(t))) \quad (14)$$

where S_{90} is a 90-degree phase-shift operator can be designed with the following transfer function:

$$HS_{90}(S) = (1 - (s / \omega_0)) / (1 + (s / \omega_0)) \quad (15)$$

By adding the PSD block with Eqs. (11)– (13) to the dqPLL structure, a PSD + dqPLL synchronization algorithm able to extract the positive sequence of the 3-phase utility grid voltages is obtained, and then, a reliable detection of the positive sequence of the frequency and phase will be achieved when voltage unbalances occur. A possible inconvenience, of the

PSD can be observed in Equation (14). The S90 phase-shift operator has been implemented using a non-adaptive nominal angular frequency ω_0 , making this filter sensible to frequency variations of the utility grid voltages, which will induce to a small degradation.

4.2. Vuvw REFERENCE GENERATOR

The reference voltage signal for generating the pulses is generated in Vuvw reference generator diagram, which is shown in figure 4 below:

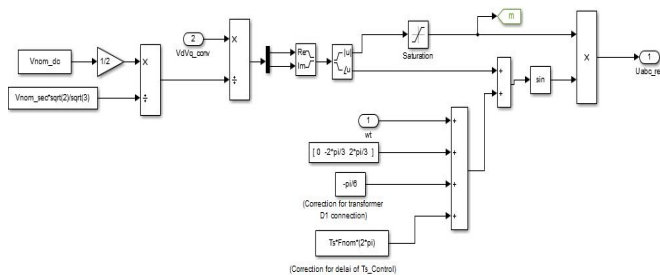


Figure 4. Vuvw reference generator diagram

5 Case of Study

A Photovoltaic grid connected system of 5 kW of nominal power at standard conditions (1000 W / m² and 25°C) will be studied in order to evaluate the control algorithms performance. MPPT is connected in the boost converter using the Perturb and Observe 'P & O' technique. The elaborate model includes the following components:

- Photovoltaic array delivering a maximum of 5 kW at 1000 W/m² sun irradiance.
- Boost converter (DC-DC) increasing voltage from Photovoltaic natural voltage (273 V DC at maximum power) to 500 V DC.

Two control loops are used to control the voltage source converter: an internal loop which allows regulated I_q and I_d , and an external loop which controls the DC link voltage to ± 250 V. I_q is set to zero to maintain the unit power factor.

Pulse generators of DC-DC and VSC converters use a fast sample time of one microsecond in order to obtain an appropriate resolution of PWM waveforms.

6. Results and Analysis

Figure 5 shows the SIMULINK model of the proposed system, where a discrete model is used for the Plant with a sample time of 50 μ s.

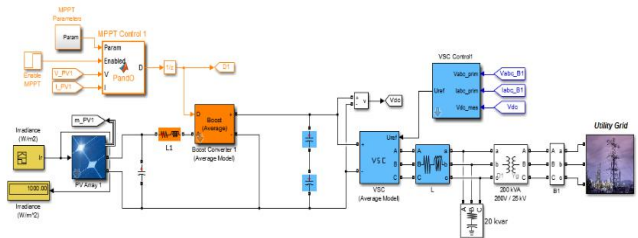


Figure 5. SIMULINK model of the grid-connected PV system.

The boost converter amplifies the DC voltage from 273.5V to 500 V. To obtain the maximum power we used an MPPT command based on the P & O algorithm, we varied D. In order to control the system, two control loops have been used, an external loop which makes it possible to regulate the direct voltage to the grid currents I_d and I_q . The output of the external controller represents an identity current reference. I_q is the current reference set to zero to maintain the unit power factor. The control system as well as the synchronization unit uses a sampling time of 100 controller.

Running Simulink on the MATLAB platform for a period of 3 seconds the following is observed (Figure 6).

From $t=0$ s to $t= 0.05$ s, pulses to DC-DC and VSC converters are blocked. PV voltage corresponds to open-circuit voltage ($N_{ser} \cdot V_{oc} = 5 \cdot 64.2 = 321$ V, see V trace on Scope Boost Figure 6). The three level bridge function as a diode rectifier and DC link capacitors are charged above 500 V (see Vdc_meas trace on Scope VSC).

At $t=0.05$ s, Boost and VSC converters are de regulated at $V_{dc}=500$ V. Duty cycle of DC-DC converter is fixed ($D= 0.5$ figure 7) and sun irradiance is fixed to 1000 W/m².

Stable at $t=0.25$ s. Resulting Photovoltaic voltage is therefore $V_{PV} = (1 - 0.5) \cdot 500 = 250$ V (see V trace on Scope Boost). The Photovoltaic array output power is 4.5 kW (see Pmean trace on Scope Boost converter).

At $t = 0.4$ s, the maximum power point tracker is activated. At time $D = 0.453$. At $t = 0.6$ s, the MPP is obtained ($P_{max} = 5$ KW).

From $t = 0.7 \text{ s}$ to $t = 1.2 \text{ s}$, the irradiance of the sun is reduced from 1000 W / m^2 to 250 W / m^2 . the Maximum power point tracker continues tracking maximum power. At $t=1.2 \text{ s}$ when irradiance has diminished to 250 W/m^2 , duty cycle is $D=0.485$. Corresponding PV voltage and power are $V_{\text{mean}}=255 \text{ V}$ and $P_{\text{mean}}=1.2 \text{ kW}$. Note that the MPPT continues tracking maximum power during this fast irradiance.

From $t=1.5 \text{ s}$ to 3 s various irradiance changes are applied in order to illustrate the nice performance of the MPPT controller.

In Figure 7 present the reponse of voltage source converter. A typical situation in Photovoltaic systems is a variation of the solar irradiance over the Photovoltaic modules due to clouds or a sunny day: Figure 8 and figure 9. shows the time simulation of a variation in the incoming irradiance. for that, a step in the output current of the Photovoltaic generator is exerted at 0.05 s from a 50% up to nominal conditions with constant dc bus voltage reference.

FIG. 9 shows the evolution of the utility network current time in phase 1, thus increasing the current can be observed.

The simulation of the time evolution of the detected frequency and phase, utilizing the dqPLL and the PSD + dqPLL synchronization algorithms are shown in Figure 11. The rms value of the 3-phase utility grid voltage is $V_{\text{rms}}= 500 \text{ V}$ (phase-to-phase) and a step of frequency from 50 Hz to 60 Hz is exerted at 0.05 s . The frequency detection by two algorithms is shown in Figure 11; even though the S90 filter has been elaborated for a nominal frequency of 50 Hz , a similar response to the dqPLL is attained. admissible phase detection is attained by the PSD + dqPLL, but it must be pointed out that a small lag between the detected phases can be observed.

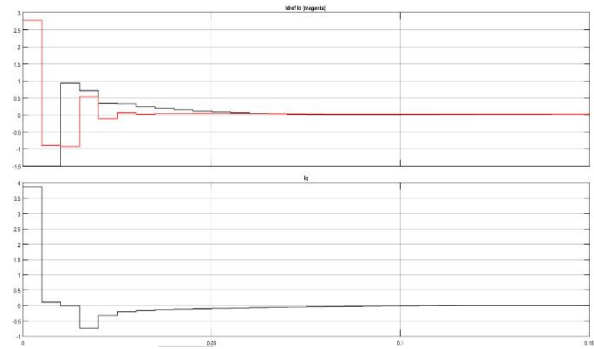


Figure 7. Response of Voltage Source Converter

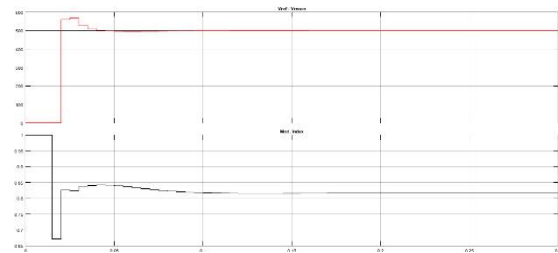


Figure 8. Response of Voltage Source Converter Waveform for Modulation Index and Inverter

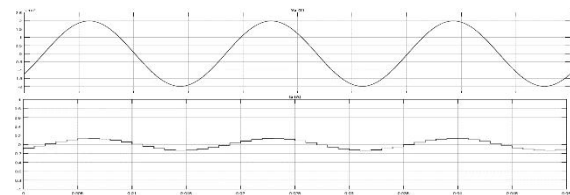


Figure 9. grid voltage and current

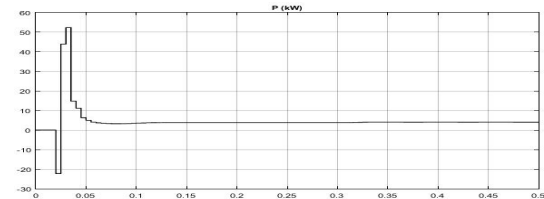


Figure 10. Synchronized Grid Power

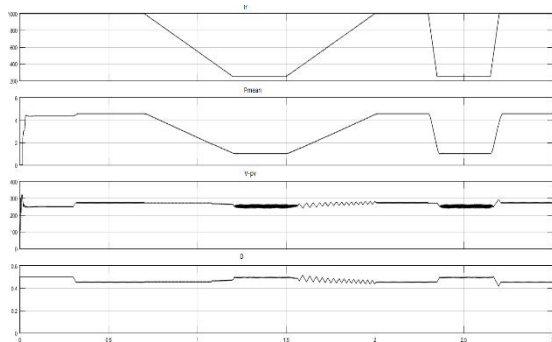


Figure 6. Waveforms of Boost Converter: Ir, Pmean, Vpv, D

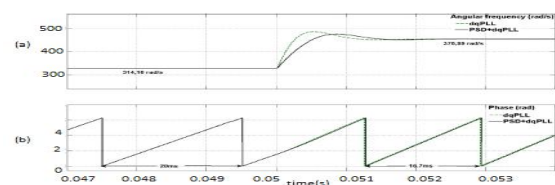


Figure 11. Time evolution of the detected frequency and phase when a step of frequency is exerted.

7 Conclusion

In the present study, we have modeled and simulated all the equipment representing the PV system connected to the electrical network, control and connection of the electrical network is ensured by the PSD algorithm plus the synchronization algorithm (dqPLL) The performance of this algorithm evaluates the synchronization behavior, introducing several perturbations in the three-phase service grid.

The proposed Photovoltaic system can provide enhanced active power smoothing and expanded reactive power compensation. A developed dual-stage DFT PLL was developed and implemented by the Photovoltaic System. The validation of the results is obtained by the responses of the tensions, currents and powers which are obtained by simulation which are close to those presented in the literature, which makes it possible to validate our work.

References:

- [1] Bennis, G., Karim, M., & Lagrioui, A. (2015, December). Optimization of the performance of a photovoltaic system with MPPT controller. In 2015 3rd International Renewable and Sustainable Energy Conference (IRSEC) (pp. 1-6). IEEE
- [2] Ghita, B., Mohammed, K., Ahmed, L., Nada, Z., Nourddine, S., & Ayoub, E. (2016). Optimization and modeling of a given PV system has a single phase load. *Journal of Theoretical & Applied Information Technology*, 86(1).
- [3] Gao, L., Dougal, R. A., Liu, S., & Iotova, A. P. (2009). Parallel-connected solar PV system to address partial and rapidly fluctuating shadow conditions. *IEEE Transactions on industrial Electronics*, 56(5), 1548-1556.
- [4] Roman, E., Alonso, R., Ibañez, P., Elorduizapatarietxe, S., & Goitia, D. (2006). Intelligent PV module for grid-connected PV systems. *IEEE Transactions on Industrial electronics*, 53(4), 1066-1073.
- [5] Hua, C., & Shen, C. (1998, May). Study of maximum power tracking techniques and control of DC/DC converters for photovoltaic power system. In *Power Electronics Specialists Conference, 1998. PESC 98 Record. 29th Annual IEEE (Vol. 1, pp. 86-93)*. IEEE.
- [6] Molina, M. G., & Mercado, P. E. (2008, August). Modeling and control of grid-connected photovoltaic energy conversion system used as a dispersed generator. In *Transmission and Distribution Conference and Exposition: Latin America, 2008 IEEE/PES (pp. 1-8)*. IEEE.
- [7] Zhou, K., & Wang, D. (2002). Relationship between space-vector modulation and three-phase carrier-based PWM: a comprehensive analysis [three-phase inverters]. *IEEE transactions on industrial electronics*, 49(1), 186-196.
- [8] A.B. Rey-Boué, R. García-Valverde, F. Ruz-Vila, J.M. Torrelo-Ponce, An inte-grative approach to the design methodology for 3-phase power conditioners in photovoltaic grid-connected systems, *Energy Convers. Manage.* 56 (2012)80–95.
- [9] H. Akagi, E. Hirokazu Watanabe, M. Aredes, *Instantaneous Power Theory and Applications to Power Conditioning*, John Wiley & Sons, New Jersey, 2007.
- [10] G. Tsengenes, G. Adamidis, Investigation of the behavior of a three phase grid-connected photovoltaic system to control active and reactive power, *Electr. Power Syst. Res.* 81 (2011) 177–184.
- [11] L. Freris, D. Infield, *Features of Conventional and Renewable Generation, Renewable Energy in Power Systems*, A John Wiley & Sons, Ltd., United King-dom, 2008, pp. 21–54.
- [12] G. Notton, V. Lazarov, L. Stoyanov, Optimal sizing of a grid-connected PV sys-tem for various PV module technologies and inclinations, inverter efficiency characteristics and locations, *Renew. Energy* 35 (2010) 541–554.
- [13] V. Scarpa, S. Buso, G. Spiazzi, Low-complexity MPPT technique exploiting the PV module MPP locus characterization, *IEEE Trans. Ind. Electron.* 56 (2009)1531–1538.
- [14] N. Mutoh, M. Ohno, T. Inoue, A method for MPPT control while searching for parameters corresponding to weather conditions for PV generation systems, in: *IECON 2004. 30th Annual Conference of IEEE. vol. 3, 2nd November, 2004, pp. 3094–3099*.
- [15] K. Zhou, D. Wang, Relationship between space-vector modulation and three-phase carrier-based PWM: a comprehensive analysis [three-phase inverters], *IEEE Trans. Ind. Electron.* 49 (2002) 186–196.
- [16] R.H. Park, Two reaction theory of synchronous machines. Generalized method of analysis – Part I, in: *Proc. Winter Convention of AIEE, 1929, pp. 716–730*.
- [17] S. Wang, C. Xu, H. Qin, Design theory and implementation of planar EMI fil-ter based on

- annular integrated inductor-capacitor unit, *Electromagn. Compat.(APEMC)* (2013) 129–132.
- [18] C. Po-Shen, L. Yen-Shin, Effective EMI filter design method for three-phase inverter based upon software noise separation, *IEEE Trans. Power Electron.* 25(2010) 2797–2806.
- [19] N.S. D’Souza, L.A.C. Lopes, X. Liu, Comparative study of variable size perturbation and observation maximum power point trackers for PV systems, *Electr. Power Syst. Res.* 80 (2010) 296–305
- [20] Choi, J. W., Kim, Y. K., & Kim, H. G. (2006). Digital PLL control for single-phase photovoltaic system. *IEE Proceedings-Electric Power Applications*, 153(1), 40-46.
- [21] Blaabjerg, F., Teodorescu, R., Liserre, M., & Timbus, A. V. (2006). Overview of control and grid synchronization for distributed power generation systems. *IEEE Transactions on industrial electronics*, 53(5), 1398-1409.
- [22] F. Blaabjerg, Z. Chen, S.B. Kjaer, Power electronics as efficient interface in dispersed power generation systems, *IEEE Trans. Power Electron.* 19 (2004) 1184–1194.
- [23] A.V. Timbus, M. Liserre, R. Teodorescu, P. Rodriguez, F. Blaabjerg, Evaluation of current controllers for distributed power generation systems, *IEEE Trans. Power Electron.* 24 (2009) 654–664.
- [24] A. Luna, J. Rocabert, I. Candela, P. Rodriguez, R. Teodorescu, F. Blaabjerg, Advanced structures for grid synchronization of power converters in distributed generation applications, in: *Energy Conversion Congress and Exposition (ECCE)*, 2012, pp. 2769–2776.
- [25] G. Bennis, M. Karim, A. Lagrioui, M. Felja, “Comparison Between the Conventional PSO Method and Modified PSO Method for PV system Under Shading,” in *WSEAS Transactions on Systems and Control*, vol 13.